

Long-lived nonequilibrium superconductivity in a noncentrosymmetric Rashba semiconductorV. Narayan,^{1,*} P. C. Verpoort,¹ J. R. A. Dann,¹ D. Backes,^{1,†} C. J. B. Ford,¹ M. Lanius,² A. R. Jalil,² P. Schüffelgen,² G. Mussler,² G. J. Conduit,¹ and D. Grützmacher²¹*Department of Physics, University of Cambridge, J. J. Thomson Avenue, Cambridge CB3 0HE, United Kingdom*²*Peter Grünberg Institute (PGI-9), Forschungszentrum Jülich & Jülich-Aachen Research Alliance (JARA-FIT), 52425 Jülich, Germany*

(Received 24 November 2018; revised manuscript received 5 April 2019; published 10 July 2019)

We report nonequilibrium magnetodynamics in the Rashba-superconductor GeTe, which lacks inversion symmetry in the bulk. We find that at low temperature the system exhibits a nonequilibrium state, which decays on timescales that exceed conventional electronic scattering times by many orders of magnitude. This reveals a nonequilibrium magnetoresponse that is asymmetric under magnetic-field reversal and, strikingly, induces a nonequilibrium superconducting state distinct from the equilibrium one. We develop a model of a Rashba system in which nonequilibrium configurations relax on a finite timescale that captures the qualitative features of the data. We also obtain evidence for the slow dynamics in another nonsuperconducting Rashba system. Our work provides insights into the dynamics of noncentrosymmetric superconductors and Rashba systems in general.

DOI: [10.1103/PhysRevB.100.024504](https://doi.org/10.1103/PhysRevB.100.024504)

Rashba systems are a class of spin-orbit coupled materials in which spatial inversion symmetry is absent and whose band structure, therefore, lacks spin degeneracy. The dispersion of Rashba systems features two concentric Fermi surfaces with opposing helical spin structures that are separated in momentum space by twice the Rashba wave vector k_R . Systems displaying a large Rashba effect are desirable for all-electrical spin-based logic schemes, and Rashba superconductors are expected to harbor topological superconducting phases [1], much sought-after toward fault-tolerant quantum computation. While the breaking of spatial inversion is most readily achieved in low-dimensional systems, recently three-dimensional materials such as bismuth tellurohalides [2] and GeTe [3] have been shown to have a giant bulk Rashba effect.

It is known that the presence or absence of specific symmetries in a system has a telling effect on the allowed dynamical processes [4]. In the specific case of Rashba systems, transitions between the two Rashba bands are constrained by the finite momentum split k_R and the helical spin-structure. As we will show in this paper, this has important consequences for equilibration. The spin structure of the Rashba bands also has important consequences for superconducting systems and, in particular, the nature of Cooper pairs [5,6]. Thus, Rashba superconductors can harbor unconventional superconducting phases including Fulde-Ferrell-Larkin-Ovchinnikov-type [7,8] phases in which the Cooper pair has a finite momentum and/or topological superconductor phases [1,9–12].

We report here low-temperature (T), magnetic-field (B)-induced dynamics in molecular-beam-epitaxy (MBE)-grown ultrathin films (18-nm-thick) of GeTe (for details of sample growth, please see Ref. [14]). GeTe is a narrow band-gap

semiconductor with giant bulk and surface Rashba couplings [3,15], and is inherently superconducting [16,17]. We present data from two Hall bar samples patterned from the same wafer (for details, see [14]), which become superconducting below 0.2 K. Strikingly, we find that a second nonequilibrium superconducting state with a higher critical temperature (T_c) and critical field (B_c) is accessed when the system is subjected to a continuously ramped magnetic field $B(t)$. This nonequilibrium state is extremely long-lived, relaxing on macroscopic timescales of several minutes. By ruling out other well-known sources of slow dynamics, we demonstrate that the mechanism underlying the observed dynamics is novel. We have shown that such long-lived nonequilibrium behavior can generically be expected in clean Rashba systems [18]: in materials with strong Rashba coupling, where k_R is much larger than the thermal phonon momentum scale, there is a suppression of all relaxation processes involving real phonon modes. Furthermore, the spin texture at the Fermi surface serves to significantly reduce the scattering events due to intercarrier interactions, ultimately resulting in nonequilibrium states with finite lifetimes. Based on this, we formulate a model of a Rashba superconductor with suppressed interband transitions, within which the nonequilibrium superconducting behavior arises from the enhancement of the density of states. Our model suggests similar dynamics in normal Rashba materials, evidence of which we observe in a topological insulator heterostructure with dominantly bulk-type transport.

Figure 1 characterizes the equilibrium electrical properties of GeTe in the normal and superconducting states. Between room T and ≈ 100 K, GeTe shows activated behavior indicative of a band gap of 0.1 eV. Below 100 K the transport becomes T -independent, suggesting the role of two-dimensional (2D) modes. Correspondingly, the electrical characteristics are plotted as “sheet resistances” defined as $R \times W / L$, where R is the electrical resistance measured using a constant-current, four-terminal setup, and W and L are the width and length of the Hall bar. The 2D nature of transport is

*Author to whom all correspondence should be addressed: vn237@cam.ac.uk

†Present address: Department of Physics, Loughborough University, Loughborough LE11 3TU, United Kingdom.

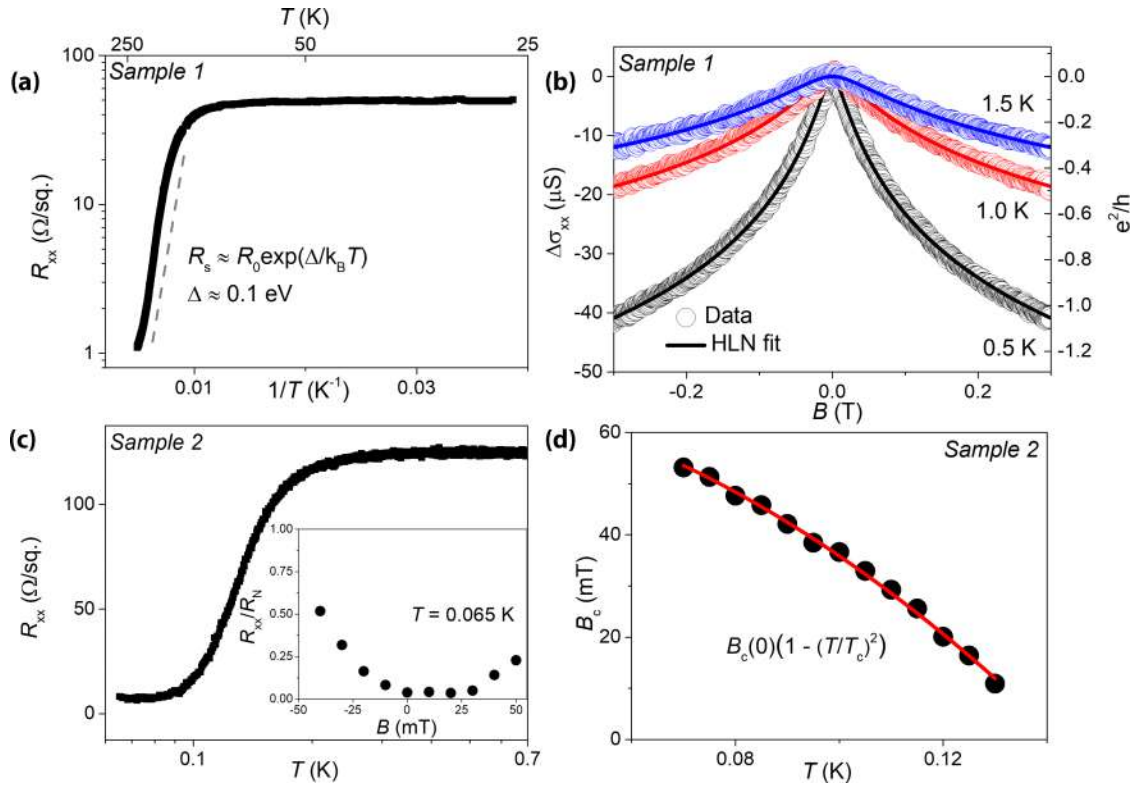


FIG. 1. GeTe: a semiconducting, spin-orbit-coupled superconductor. (a) The ultrathin GeTe films show semiconducting characteristics at high T with a band gap of ≈ 0.1 eV. Below 100 K, the T dependence weakens significantly, being indicative of 2D metallic states. (b) The spin-orbit coupling in GeTe manifests as WAL, i.e., positive quantum corrections to the electrical conductivity $\Delta\sigma_{xx} = \sigma_{xx}(B) - \sigma_{xx}(0)$. These characteristics are well described by the Hikami-Larkin-Nagaoka (HLN) [13] formula valid for 2D systems (see also Fig. S2 [14]). (c) There is a broad superconducting transition between 0.2 and 0.1 K below which we note that R_{xx} does not go completely to zero (see Fig. S3 [14] for possible explanation). Inset: superconductivity is suppressed when the sample is cooled in the presence of a constant magnetic field perpendicular to the plane of the film. The data are consistent with a field offset of ≈ 15 mT, which can arise due to trapped flux in the external superconducting magnet (see Fig. S4 [14] for details of how these data are collected). (d) The dependence of the critical field B_c on T reveals $B_c(0 \text{ K}) = 70$ mT and $T_c = 140$ mK. Here the superconducting transition is defined as $R_{xx} < R_N/2$ (where R_N is the normal-state resistance).

corroborated by the low- T magnetotransport, where positive quantum corrections to the electrical conductivity σ_{xx} or weak antilocalization (WAL) characteristics are seen to be 2D-like [Fig. 1(b), Fig. S2 [14]]. Here $\sigma_{xx} \equiv (L/W)R_{xx}/(R_{xx}^2 + R_y^2)$, where R_{xx} and R_y are the longitudinal and Hall components of resistance, respectively. For reasons that will become apparent later in the paper, while recording the data in Fig. 1(b) the magnitude of the magnetic field was kept to less than 0.3 T [14] at all times. The observation of 2D modes is consistent with recent spectroscopic measurements [15], although our results are not affected by the dimensionality of transport. Figure 1(c) shows the onset of the superconductivity at $T = 0.2$ K and its suppression under the influence of a perpendicular magnetic field (B).

Evidence of a second *nonequilibrium* superconducting state is shown in Fig. 2. Under the influence of a slowly ramped B field perpendicular to the plane of the sample, it is found that [Figs. 2(a)–2(c)] (i) superconductivity is no longer observed at $B = 0$ T, but instead appears at a finite B ; (ii) the magnetoresistance is asymmetric about the new superconducting state, depending explicitly on the sign of dB/dt ; and (iii) the nonequilibrium state is highly persistent, relaxing on the timescale of minutes [Fig. 2(d) and Fig. S5 [14]]. The occurrence of this state relies on a finite dB/dt

without which one obtains the “equilibrium” magnetoresistance [Fig. 1(c), inset]. Strikingly, however, Fig. 2(e) shows that sweeping at a slower rate serves to enhance the finite- B minimum (R_{\min}), implicating an optimum sweep rate at which the nonequilibrium superconducting state manifests most clearly. The enhancement of B_c evidenced in Figs. 2(a)–2(c) in conjunction with the behavior in Fig. 2(d) strongly suggests that the dynamical superconducting state is distinct from the initial equilibrium superconducting state, and results from a long-lived transient configuration. This is supported by Figs. 2(f)–2(i) (and Fig. S7 [14]), where we find that its existence is not contingent on the equilibrium superconducting state, occurring even above T_c and remaining perceptible up to $T = 0.4$ K. The absence of complete loss of resistance could be interpreted as a competition of the timescales for the transition into the superconducting phase, and the decay of the nonequilibrium state (see Fig. S5 [14]).

There are various mechanisms that are known to result in slow relaxation in solid-state systems. In the supplemental material [14], we discuss and rule out contributions due to magnetocaloric effects, superconducting vortices, nuclear spins, trapped flux, and inhomogeneities in the GeTe film. We also note that the recent findings of “nonreciprocal transport” in Rashba systems [19,20] cannot explain our experimental

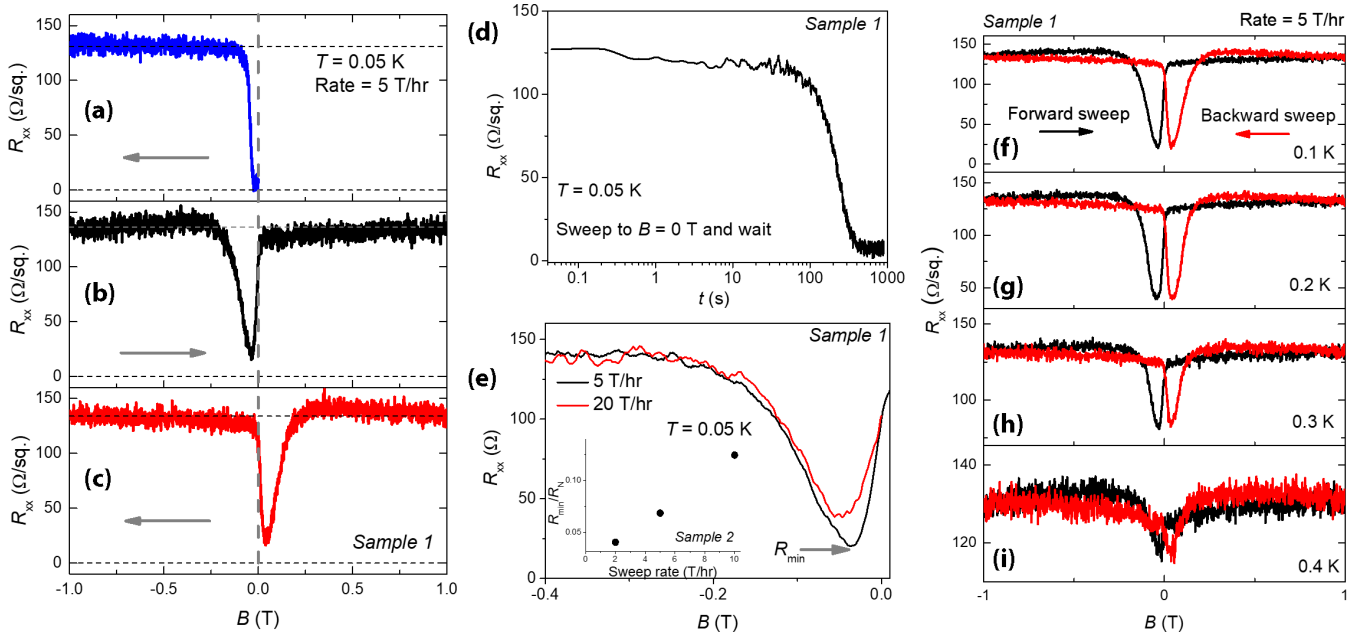


FIG. 2. Long-lived nonequilibrium magnetodynamics. (a) Starting in the superconducting state, as B is ramped toward -1 T at $dB/dt = 5$ T h $^{-1}$ (1.4 mT s $^{-1}$), there is a sharp transition to the normal state at -15 mT. However, the “forward B sweep” from -1 to 1 T shown in (b) is distinctly dissimilar to the previous trace, showing an initial increase in R_{xx} followed by an almost complete transition to superconductivity beginning at $B = -250$ mT, well above the previously estimated values of B_c . The sweep is not symmetric about R_{\min} or about $B = 0$ T. In contrast, at $B = 0$ T, the value R_{xx} is now finite and close to R_N . (c) The shape of R_{xx} as B is swept in the opposite direction from 1 to -1 T is precisely the mirror image of the forward sweep when reflected about $B = 0$ T. The gray arrows indicate the direction of the B sweep. (d) When the sweep is stopped at $B = 0$ T the nonequilibrium state persists for ≈ 100 s before relaxing to the equilibrium zero-resistance state over a further 300 s. (e) Over the range of sweep rates explored, R_{xx} is seen to show a lower minimum R_{\min} for slower sweep rates. Inset: R_{\min}/R_N as a function of sweep rate. (f)–(i) The apparent nonequilibrium superconducting state is visible even above T_c .

observations as these are equilibrium effects. In particular, we find no violation of reciprocity in the equilibrium transport [Fig. 1(c), inset].

In Ref. [18], we explicitly consider the relaxation dynamics in Rashba-coupled systems and establish that in the absence of charged impurities and below a characteristic T , nonequilibrium configurations relax on timescales that can be many orders of magnitude greater than the conventionally observed picosecond relaxation timescales. For GeTe we show that this characteristic T can be as large as 1 K. In the following, we verify whether the existence of such a timescale is a sufficient condition to induce the observed novel magnetoresponse by considering a model Rashba superconductor and introducing, by hand, a finite timescale τ for interband transitions. We estimate $\tau \sim 100$ s for the GeTe films from Fig. S5(a) [14,21].

The Rashba dispersion is given by $\epsilon_k^\pm = \hbar^2 \mathbf{k}^2 / 2m \pm \sqrt{(g\mu_B B)^2 + (\alpha_R \mathbf{r}_{SO} \times \mathbf{k})^2}$, where the $+$ ($-$) superscript refers to the inner (outer) Rashba band. Here, \hbar is Planck’s constant, \mathbf{k} is the wave vector, m is the effective mass of carriers, g is the Landé g -factor, μ_B is the Bohr magneton, α_R is the Rashba parameter, and \mathbf{r}_{SO} is the direction of the spin-orbit coupling along which inversion symmetry is broken. This assumes the direction of the B field to lie parallel to \mathbf{r}_{SO} (however, this assumption does not affect the qualitative results as in-plane fields cause a redistribution of carriers between bands similar to the out-of-plane one). To study the consequences of the time-varying magnetic field, we compute the dynamical Fermi energies ϵ_F^\pm as a function of

time t , whose time dependence is governed by the differential equation:

$$\frac{d\epsilon_F^\pm}{dt} = \frac{\partial \epsilon_F^\pm}{\partial B} \frac{\partial B}{\partial t} + \frac{\partial \epsilon_F^\pm}{\partial n^\pm} \frac{\partial n^\pm}{\partial t}, \quad (1)$$

where n^\pm are the carrier densities of the two bands. The first term on the right describes how the Fermi surfaces change with B and the second term describes carriers relaxing so as to equilibrate ϵ_F^+ and ϵ_F^- . We model $\frac{\partial n^\pm}{\partial t}$ using a relaxation-time approximation with time constant τ . To describe the superconductivity, we make the following generic assumptions: (i) superconductivity is assumed to emerge through pairing of opposite spin carriers within a band (this is the simplest prescription based on Cooper pairs with zero net momentum [22], and while it is assumed for simplicity, the model is readily extended to include interband Cooper pairing); (ii) the transition temperature T_c [23] is assumed to depend exponentially on the density of states ν : $T_{c\pm} \sim e^{(-1/\Gamma \nu_\pm)}$, where the \pm indicate the two Rashba bands, $\nu_\pm \sim \frac{dk}{d\epsilon_\pm}$, and Γ is the strength of the contact interaction that mediates superconductivity. Γ is drawn from a uniform probability distribution to reflect local variations in dopant concentration, interaction strength, etc. The magnetoresistance is modeled by $R = R_N \min(T/T_{c-}, 1)$, which arises only from the parts of the sample that are normal. The results of our model calculation are shown in Fig. 3(a), and they capture the essential features of the experimental observations in Figs. 2(a)–2(c) and 2(f)–2(i). Notably, this simple model does not capture the dB/dt dependence of the

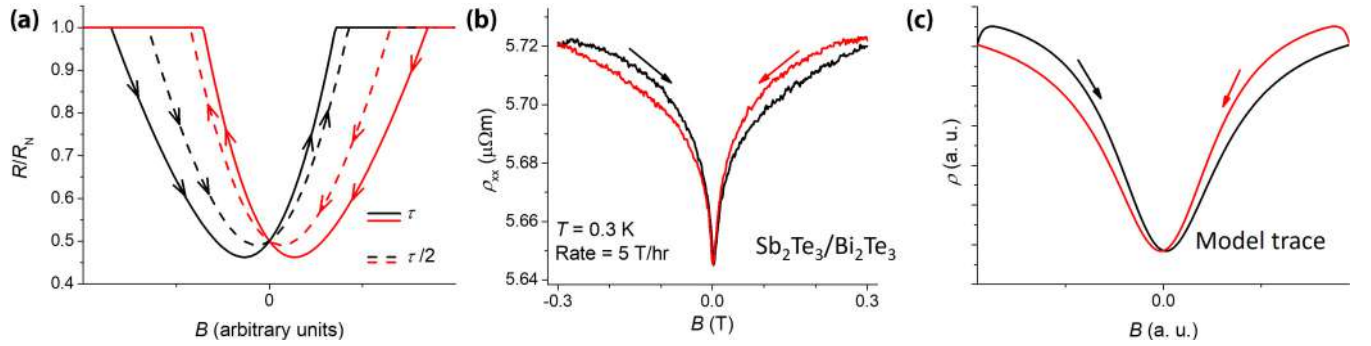


FIG. 3. Nonequilibrium butterfly hysteresis. (a) The magnetoresistance of a model Rashba system subjected to a B field, in which interband relaxation processes occur on a finite timescale τ . The two traces compare the behavior when τ is changed by a factor of 2. Superconductivity is induced locally depending on the instantaneous carrier concentration. The model correctly captures the difference between traces with differing sign of dB/dt as well as $R(B) \neq R(-B)$ for a given sign of dB/dt . (b) The asymmetric $\rho(B)$ and mirror symmetry between the forward and reverse B sweeps are clearly seen in a heterostructure of p - and n -type topological insulators. (c) The characteristic “butterfly” shape of $\rho(B)$ can be captured within a model of a Rashba material.

depth of the dip [Fig. 2(e)], which is likely a higher-order effect requiring a more microscopic treatment. One plausible scenario is that the nonequilibrium superconducting state has a more complex history dependence (Fig. S10 [14]) or involves interband Cooper pairing and thus requires a threshold occupancy in both Rashba bands.

It is noteworthy that the arguments of long relaxation times presented in Ref. [18] are generic to Rashba systems as opposed to only Rashba superconductors. In this context, we first point out that the novel asymmetric and rate-dependent magnetodynamics are observed in GeTe even in samples that do not go superconducting [17]. Figure 3(b) demonstrates similar, albeit less pronounced, qualitative features in a vertical topological insulator (TI) p - n junction [24–26] in which a 6 nm layer of Bi_2Te_3 is capped with a 15 nm layer of Sb_2Te_3 . Here transport is in the plane of the film and B is out of plane. TIs are well-known spin-orbit materials, and the in-built potential of the p - n junction [24] provides a clear mechanism for the breaking of inversion symmetry. Importantly, the specific layer configuration is known to show significant bulk transport [25] rather than the surface-dominated transport in ultrathin TIs, where this effect is not expected due to the single Dirac cone. We stress that this behavior should not be confused with the so-called “butterfly hysteresis” observed in magnetic Dirac materials [27–32] since (i) the materials reported here are manifestly nonmagnetic, and (ii) the data reflect nonequilibrium states in the samples.

Figure 3(c) shows the qualitative behavior of $\rho(B) \approx \frac{1}{(\sigma^+ + \sigma^-)}$ as derived from the conductivities $\sigma^\pm \propto \int dk 3 \left(\frac{\partial \epsilon_{\mathbf{k}}^\pm}{\partial k} \right)^2 \delta(\epsilon_{\mathbf{k}}^\pm - \epsilon_{\text{F}}^\pm)$ of the bands and the dynamics of $\epsilon_{\text{F}}^\pm(t)$ arising due to Eq. (1), evaluated for a parabolic band dispersion. The figure clearly captures the salient features of the experimental data (although for a quantitative comparison, in addition to realistic band structure, one also needs to account for WAL corrections to the conductivity). The physical mechanism is the exact same as before: the two Rashba bands develop unequal Fermi levels when subjected to a B sweep. Since changes in conductivity of the two bands do not cancel, i.e., $\frac{\partial \sigma^+}{\partial n^+} \neq \frac{\partial \sigma^-}{\partial n^-}$, there is a net change in the total conductivity $\sigma^+ + \sigma^-$.

For the parabolic dispersion considered in our model, the sweep toward zero field has a higher resistance than the sweep away from zero (corresponding to the black trace being higher than the red trace for $B < 0$ T) and the minimum in the magnetoresistance occurs after crossing $B = 0$ T. This completely agrees with the behavior seen in the TI heterostructure [Fig. 3(b)], but the latter characteristic is different from that seen in GeTe (Fig. 2) where the minimum occurs before crossing $B = 0$ T. This difference stems purely from the superconductivity in GeTe and is well-captured in our model shown in Fig. 3(a). Lastly, we stress that while GeTe shows a dramatic magnetoresponse, this can be much more subtle, as shown in Fig. 3(b). We question whether similar observations may have been overlooked in the past.

In conclusion, we have reported ultraslow relaxation and rich nonequilibrium magnetodynamics in the noncentrosymmetric Rashba superconductor GeTe. These dynamics reveal a second nonequilibrium superconducting state with a higher T_c and B_c . Importantly, the observed slow dynamics are inconsistent with more common sources of slow dynamics such as nuclear spin relaxation and vortex creep. They are also inconsistent with magnetocaloric-driven cooling and/or eddy current-induced heating. We develop a model that successfully captures the salient features of the experimental data, and also predicts a specific response in normal Rashba systems, qualitative evidence of which we observe in a TI-based heterostructure. We suggest, therefore, that our observations might be generic to Rashba systems, and we discuss the conditions under which they might be observed in experiment. Our work has provided striking experimental insights into the behavior of Rashba superconductors and possibly indicates a nonequilibrium behavior unique to Rashba systems in general.

V.N., J.R.A.D., P.C.V., D.B., and C.J.B.F. acknowledge funding from the Engineering and Physical Sciences Research Council (EPSRC), UK. G.J.C. acknowledges funding from the Royal Society, UK. G.M., M.L., A.R.J., P.S., and D.G. acknowledge financial support from the DFG-funded priority programme SPP1666 as well as from the Helmholtz Association via the “Virtual Institute for Topological Insulators”

(VITI). V.N. acknowledges useful discussions with Mark Blamire, Siddharth Saxena, Niladri Banerjee, Peter Wahl, and Yoichi Ando. V.N. also thanks Seamus Davis for suggesting the measurements in Fig. S9 [14]. P.C.V. acknowledges useful discussions with Giulio Schober.

There is Open Access to this paper and data available at Ref. [35].

V.N. fabricated and measured the GeTe devices, and wrote the paper with inputs from P.C.V., J.R.A.D., C.J.B.F., G.M., and G.J.C. D.B. fabricated and measured the topological insulator devices. M.L., A.R.J., P.S., G.M., and D.G. grew and characterized the GeTe films and topological insulator heterostructures. P.C.V. and G.J.C. performed the theoretical modeling.

- [1] M. Sato and S. Fujimoto, *Phys. Rev. B* **79**, 094504 (2009).
- [2] B. M. Saeed and N. Ogawa, *Adv. Mater.* **29**, 1605911 (2017).
- [3] D. D. Sante, B. Paolo, B. Riccardo, and P. Silvia, *Adv. Mater.* **25**, 509 (2012).
- [4] V. Narayan, S. Ramaswamy, and N. Menon, *Science* **317**, 105 (2007).
- [5] E. Bauer, *Non-Centrosymmetric Superconductors: Introduction and Overview*, Lecture Notes in Physics Vol. 847 (Springer, Berlin, 2012).
- [6] L. P. Gor'kov and E. I. Rashba, *Phys. Rev. Lett.* **87**, 037004 (2001).
- [7] P. Fulde and R. A. Ferrell, *Phys. Rev.* **135**, A550 (1964).
- [8] A. Larkin and I. Ovchinnikov, *Sov. Phys. JETP* **20**, 762 (1965).
- [9] F. F. Tafti, T. Fujii, A. Juneau-Fecteau, S. René de Cotret, N. Doiron-Leyraud, A. Asamitsu, and L. Taillefer, *Phys. Rev. B* **87**, 184504 (2013).
- [10] Y. Nakajima, R. Hu, K. Kirshenbaum, A. Hughes, P. Syers, X. Wang, K. Wang, R. Wang, S. R. Saha, D. Pratt, J. W. Lynn, and J. Paglione, *Sci. Adv.* **1**, e1500242 (2015).
- [11] M. Sato and Y. Ando, *Rep. Prog. Phys.* **80**, 076501 (2017).
- [12] H. Xiao, T. Hu, W. Liu, Y. L. Zhu, P. G. Li, G. Mu, J. Su, K. Li, and Z. Q. Mao, *Phys. Rev. B* **97**, 224511 (2018).
- [13] S. Hikami, A. I. Larkin, and Y. Nagaoka, *Prog. Theor. Phys.* **63**, 707 (1980).
- [14] See Supplemental Material at <http://link.aps.org/supplemental/10.1103/PhysRevB.100.024504> for sample growth and characterisation, discussion of other possible sources of slow dynamics in condensed matter systems, and additional time-dependent and magnetic field data.
- [15] M. Liebmann, C. Rinaldi, D. Di Sante, J. Kellner, C. Pauly, R. N. Wang, J. E. Boschker, A. Giussani, S. Bertoli, M. Cantoni, L. Baldrati, M. Asa, I. Vobornik, G. Panaccione, D. Marchenko, J. Sánchez-Barriga, O. Rader, R. Calarco, S. Picozzi, R. Bertacco, and M. Morgenstern, *Adv. Mater.* **28**, 560 (2016).
- [16] R. A. Hein, J. W. Gibson, R. Mazelsky, R. C. Miller, and J. K. Hulm, *Phys. Rev. Lett.* **12**, 320 (1964).
- [17] V. Narayan, T.-A. Nguyen, R. Mansell, D. A. Ritchie, and G. Mussler, *Phys. Status Solidi–Rapid Res. Lett.* **10**, 253 (2016).
- [18] P. C. Verpoort and V. Narayan, [arXiv:1902.04678](https://arxiv.org/abs/1902.04678).
- [19] R. Wakatsuki, Y. Saito, S. Hoshino, Y. M. Itahashi, T. Ideue, M. Ezawa, Y. Iwasa, and N. Nagaosa, *Sci. Adv.* **3**, e1602390 (2017).
- [20] S. Hoshino, R. Wakatsuki, K. Hamamoto, and N. Nagaosa, *Phys. Rev. B* **98**, 054510 (2018).
- [21] A stringent requirement for the slow relaxation is that no charged impurities be present. In this context, it is well known that GeTe has spontaneously formed Ge vacancies that impart it a p -type conductivity. However, these vacancies are uncharged [33,34], and therefore they do not act as charged scattering centers.
- [22] M. Smidman, M. B. Salamon, H. Q. Yuan, and D. F. Agterberg, *Rep. Prog. Phys.* **80**, 036501 (2017).
- [23] E. Lake, C. Webb, D. A. Pesin, and O. A. Starykh, *Phys. Rev. B* **93**, 214516 (2016).
- [24] M. Eschbach, E. Młyńczak, J. Kellner, J. Kampmeier, M. Lanius, E. Neumann, C. Weyrich, M. Gehlmann, P. Gospodarič, S. Döring, G. Mussler, N. Demarina, M. Luysberg, G. Bihlmayer, T. Schäpers, L. Plucinski, S. Blügel, M. Morgenstern, C. M. Schneider, and D. Grützmacher, *Nat. Commun.* **6**, 8816 (2015).
- [25] D. Backes, D. Huang, R. Mansell, M. Lanius, J. Kampmeier, D. Ritchie, G. Mussler, G. Gumbs, D. Grützmacher, and V. Narayan, *Phys. Rev. B* **96**, 125125 (2017).
- [26] D. Backes, D. Huang, R. Mansell, M. Lanius, J. Kampmeier, D. Ritchie, G. Mussler, G. Gumbs, D. Grützmacher, and V. Narayan, *Phys. Rev. B* **99**, 125139 (2019).
- [27] S. Wolgast, Y. S. Eo, T. Öztürk, G. Li, Z. Xiang, C. Tinsman, T. Asaba, B. Lawson, F. Yu, J. W. Allen, K. Sun, L. Li, Ç. Kurdak, D.-J. Kim, and Z. Fisk, *Phys. Rev. B* **92**, 115110 (2015).
- [28] A. Brinkman, M. Huijben, M. van Zalk, J. Huijben, U. Zeitler, J. C. Maan, W. G. van der Wiel, G. Rijnders, D. H. A. Blank, and H. Hilgenkamp, *Nat. Mater.* **6**, 493 (2007).
- [29] Y. Nakajima, P. Syers, X. Wang, R. Wang, and J. Paglione, *Nat. Phys.* **12**, 213 (2015).
- [30] G. N. Daptary, S. Kumar, A. Bid, P. Kumar, A. Dogra, R. C. Budhani, D. Kumar, N. Mohanta, and A. Taraphder, *Phys. Rev. B* **95**, 174502 (2017).
- [31] K. L. Tiwari, W. A. Coish, and T. Pereg-Barnea, *Phys. Rev. B* **96**, 235120 (2017).
- [32] T.-A. Nguyen, D. Backes, and A. Singh, R. Mansell, C. Barnes, D. A. Ritchie, G. Mussler, M. Lanius, D. Grützmacher, V. Narayan, *Sci. Rep.* **6**, 27716 (2016).
- [33] A. H. Edwards, A. C. Pineda, P. A. Schultz, M. G. Martin, A. P. Thompson, and H. P. Hjalmarson, *J. Phys.: Condens. Matter* **17**, L329 (2005).
- [34] A. H. Edwards, A. C. Pineda, P. A. Schultz, M. G. Martin, A. P. Thompson, H. P. Hjalmarson, and C. J. Umrigar, *Phys. Rev. B* **73**, 045210 (2006).
- [35] <https://www.openaccess.cam.ac.uk/>.